Direct Wavelength-Selective Optical and Electron-Beam Lithography of Functional Inorganic Nanomaterials

Yuanyuan Wang,[†,§] Jia-Ahn Pan,[†,§] Haoqi Wu,[†] and Dmitri V. Talapin*[,†,‡]

† *Department of Chemistry and James Franck Institute, University of Chicago, Chicago, Illinois 60637, United States*

‡ *Center for Nanoscale Materials, Argonne National Laboratory, Argonne, Illinois 60439, United States*

*To whom correspondence should be addressed. E-mail: dvtalapin@uchicago.edu

§ These authors contributed equally

Abstract:

Direct optical lithography of functional inorganic nanomaterials (DOLFIN) is a photoresist-free method for high-resolution patterning of inorganic nanocrystals (NCs) that has been demonstrated with deep UV (DUV, 254 nm) photons. Here, we expand the versatility of DOLFIN by designing a series of photochemically active NC surface ligands for direct patterning using various photon energies including DUV, near-UV (i-line, 365 nm), blue (h-line, 405 nm) and visible (450 nm) light. We show that the exposure dose for DOLFIN can be ~30 mJ/cm^2, which is small compared to most commercial photopolymer resists. Patterned nanomaterials can serve as highly robust optical diffraction gratings. We also introduce a general approach for resist-free direct electron-beam lithography of functional inorganic nanomaterials (DELFIN) which enables all-inorganic NC patterns with feature size down to 30 nm, while preserving the optical and electronic properties of patterned NCs. The designed ligand chemistries and patterning techniques offer a versatile platform for nano- and micron-scale additive manufacturing, complementing the existing toolbox for device fabrication.

Keywords: inorganic nanomaterials, ligand design, photosensitive, direct patterning, photolithography, e-beam lithography.

Colloidal nanocrystals (NCs), with their size-tunable bandgaps, special light absorption and emission properties, and ease of processing,[1-3] are actively used for thin-film devices,[4-6] including the active components of field-effect transistors (FETs),[7] photodetectors,[8] LEDs,[9] solar cells[10] and optical gain materials.[11] However, current research mostly focuses on performance of individual devices, while real-world applications require co-integration of multiple components in complex device architectures, such as electronic circuits,[12] biosensor arrays,[13] and quantum dot (QD) LED displays.[14] Therefore, efficient patterning techniques for inorganic nanomaterials need to be developed.[15]

Several NC patterning techniques, including photolithography,[16] transfer printing,[14] inkjet printing,[17] screen printing[18] and laser writing[19] have been studied to optimize the resolution, throughput, fidelity, and cost per patterned element. Electron-beam lithography (EBL) allows generating patterns with very high resolution.[20,21] The above methods use colloidally-synthesized NCs capped with long-chain organic ligands, often blended with organic polymers. Unfortunately, these organic additives act as insulating barriers that impede charge or heat transport between NCs,[22] which is a critical problem for solid-state device applications. In the case of infrared optoelectronics, the organic additives also contribute to parasitic absorption and non-radiative exciton recombination.[23,24]

Among all patterning techniques, photolithography is most established for high-resolution, high-fidelity integration and manufacturing (Scheme 1, top). It enables fabrication of incredibly complex patterns for the electronics industry at very moderate costs. Traditional photolithography was originally developed and optimized for silicon integrated circuits; it has been extended to other areas, but with some technical limitations. For example, additive pattern transfers work well with gas-phase deposition methods, such as vacuum evaporation,[25] sputtering,[26] atomic layer deposition (ALD),[27] or chemical vapor deposition.[28] In all these techniques, the deposited material has very low lateral mobility, enabling the deposition of a layer with very uniform thickness. However, additive patterning of solution-processed NCs using photopolymer masks is difficult because of local capillary forces that induce lateral solvent flows leading to a non-uniform thickness of patterned layers.[29] In addition, polymers have a tendency to swell in the presence of solvents, which compromises pattern resolution.[30] These problems

motivate us to develop photosensitive NC inks for photoresist-free optical lithography of solution-processed functional materials.

Scheme 1. Outline of the processing steps for traditional photopolymer lithography (top), direct optical lithography of functional inorganic nanomaterials (DOLFIN, middle), and direct E-beam lithography of functional inorganic nanomaterials (DELFIN, bottom).

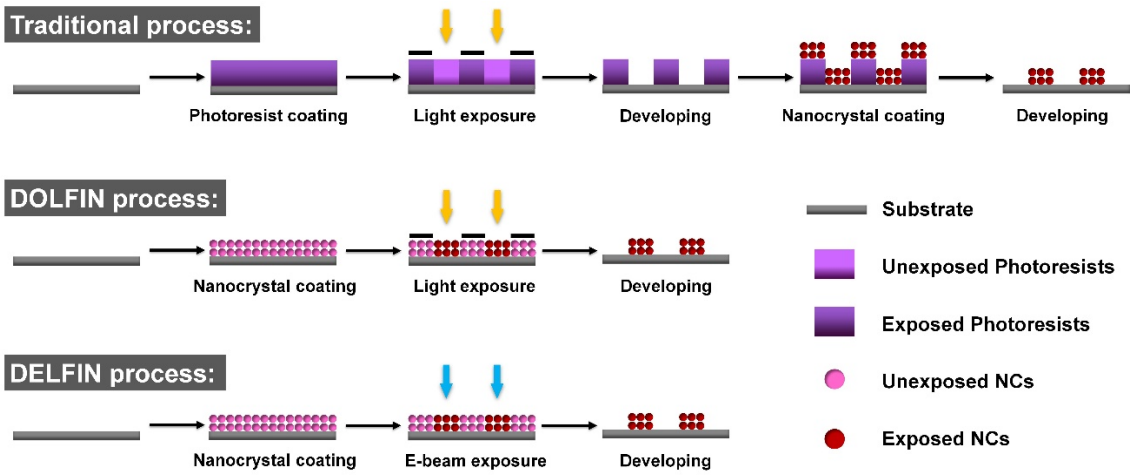

Manna and coworkers reported a photoresist-free method to pattern colloidal NCs through direct e-beam (electron beam) writing and cation exchange.[31] The high energy beam caused cross-linking of the organic ligands on NC surface which then inhibited a following cation exchange process. This method was also successfully used to pattern perovskite nanocrystal films in their later work.[32] Our team reported a different photoresists-free technique for direct optical patterning of functional inorganic materials, DOLFIN (Scheme 1, middle).[33] This strategy uses compact photosensitive surface ligands that provide colloidal stabilization to NCs. Upon controlled optical irradiation, these ligands undergo chemical transformations, which alter the solubility of NCs in a developer solvent.[33] In the first study, we introduced ligands only sensitive to 254 nm photons (DUV light), such as ammonium 1,2,3,4-thiatriazole-5-thiolate ($NH_4CS_2N_3$, or TTT) and diphenyliodonium (Ph_2I^+) or triphenylsulfonium (Ph_3S^+) photoacid generator (PAG) cations combined with the inorganic surface binding anions (*e.g.*, $ZnCl_4^{2-}$, $Sn_2S_6^{4-}$, *etc.*). We showed that almost every functional inorganic NC could be precisely patterned by DUV photons using polar developing solvents.[33] At the same time, near UV (i-line, 365 nm), blue (h-line, 405 nm) and visible (450 nm) photons have higher penetration depth, are much less damaging to

patterned nanomaterials, and much less costly compared to DUV photons.[34,35] In this work we develop a series of ligand system optimized for accessibility, stability, and compatibility with various solvents and optical wavelengths, aiming at establishing DOLFIN as a versatile technological platform for real-world additive manufacturing.

The designed ligands can be categorized into two classes, bifunctional surface ligands and photochemically active additives, according to their structures and functional groups. With simple surface treatment procedures, colloidal NCs become photochemically-active and can be directly optical patterned with either DUV (254 nm) photons, near-UV (i-line, 365 nm) photons, blue (h-line, 405 nm) photons or visible (450 nm) photons, using industrially accepted solvents. We show that the exposure dose for DOLFIN can be as small as ~30 mJ/cm^2. The generality of this approach is demonstrated for a wide range of NCs, including semiconductors, metals, oxides, *etc.* These results can serve as a foundation for developing more sophisticated approaches, such as dual-tone[36] and multicolor[37] lithography. Using similar inks, we also demonstrate a method that we call direct e-beam lithography of functional inorganic nanomaterials (DELFIN) that enables patterning of all-inorganic nanomaterials with ~30 nm lateral resolution (Scheme 1, bottom).

The nanomaterials patterned with designed ligands retain their optical and electronic properties and can be further used to design electronic and optical components, *e.g.*, electrical circuits and binary diffraction gratings. Besides being used directly as an active material, the NC layers can be used as photoresists for mainstream lithography processes. As examples, Ober and coworkers demonstrated a library of inorganic-organic hybrid photoresists consisting of metal oxide cores with organic shells.[38-42] These photoresists exhibited high etch resistance and high resolution dual tone patterning with DUV and extreme-UV (EUV, 13.5 nm) exposure. Telecky and coworkers introduced dielectric metal oxide sulfate system as a inorganic hardmask for 193 nm lithography.[43] The development of all-inorganic photoresists should further improve etch resistance and other characteristics desired for mainstream lithography workflow.

Results and Discussion

Ligand Chemistry: Requirements and Candidate Selection for DOLFIN Ligands. Direct optical patterning requires optical control over the colloidal stability of nanomaterials. One approach relies on development of small-molecule surface ligands that both provide colloidal

stability and chemically transform upon exposure to optical excitation with certain photon energy (bifunctional surface ligands). Ideally, such ligands should leave no organic residue after photo exposure, thus enabling all-inorganic patterns of functional nanomaterials. The all-inorganic design is motivated by numerous studies showing utility of NCs capped with compact, inorganic surface ligands for various thin-film devices and other applications.[5,7,10,18,44,45]

The second approach to create DOLFIN inks utilizes two different molecular species to separately fulfill the above requirements: one component (ligand) stabilizes the NC colloids while the second component acts as a photochemically active additive that alters NC solubility upon irradiation. Compared with the first type of ink, this approach can offer additional flexibility. By changing the combination of two components, we can prepare various inks to satisfy special needs in term of exposure wavelength, developing solvents, *etc*.

We screened various photochemically active molecules as candidates for DOLFIN ligands. From this search, we identified ammonium dithiocarbamate (ADC), butyldithiocarbamate (DTC), 5-Mercapto-1-methyltetrazole (MTT), and potassium ethyl xanthate (PEX) for NC patterning with DUV photons. The NC inks containing ligands of ammonium 1,1-dithiooxalate (DTO), 1,3,4-thiadiazole-2,5-dithiol (TDD) or N-hydroxynaphthalimide triflate (HNT) enabled patterning with both DUV and 365 nm (i-line) light, 1,2-naphthoquinonediazide-4-sulfonyl chloride (DNQ) as an additive enabled NC inks sensitive to 365 nm (i-line) and 405 nm (h-line) photons, while 2-phenyl-2-(-5-((tosyloxy)imino)thiophen-2-ylidene)acetonitrile (PTA) was suitable for 405 (i-line) and 450 nm visible photons lithography. The chemical structures of these ligands are shown in Scheme 2. Selected molecules cleanly decompose to small, typically volatile fragments (Eqs. 1-7 and 10-11). The chemical transformation pathways are systematically studied by using FT-IR, ESI-MS and NMR methods (See Supporting Information, SI). In addition to sensitivity to different wavelengths, each ligand system has their own distinctions: DTC allows generating NC patterns using widely industrially accepted solvents like acetone; DTO ligands photo-decompose into gaseous reaction products; PEX ligands enable NC patterning with a low exposure dose of ~30 mJ/cm^2; CdSe/CdS, CdSe/ZnS and InP/ZnSe core–shell QDs retain high PL efficiency when patterned with ADC and TDD ligands. In the following section, we summarize and discuss the properties of each ligand and NC ink.

Scheme 2. Chemical structures of designed photoactive ligands used for DOLFIN. Compounds with an asterisk (*) have been first introduced in ref. [33].

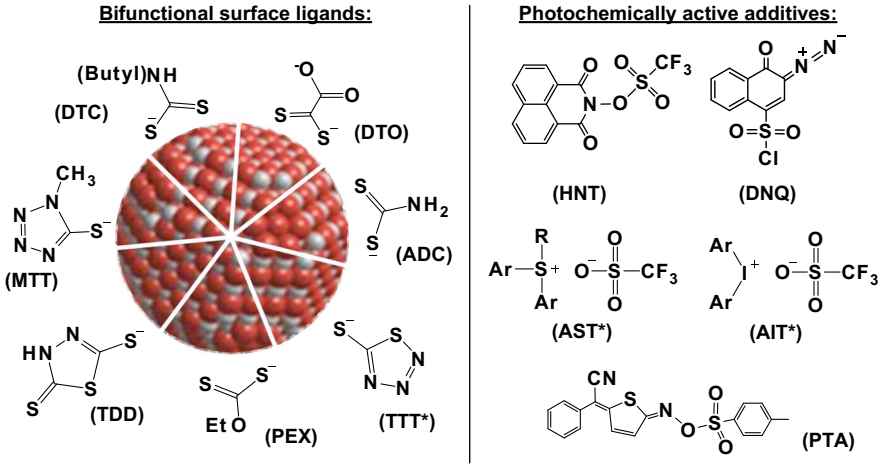

Scheme 3. Decomposition pathways of various photosensitive ligands. Additional details and mechanistic studies are provided in the Supplementary Information.

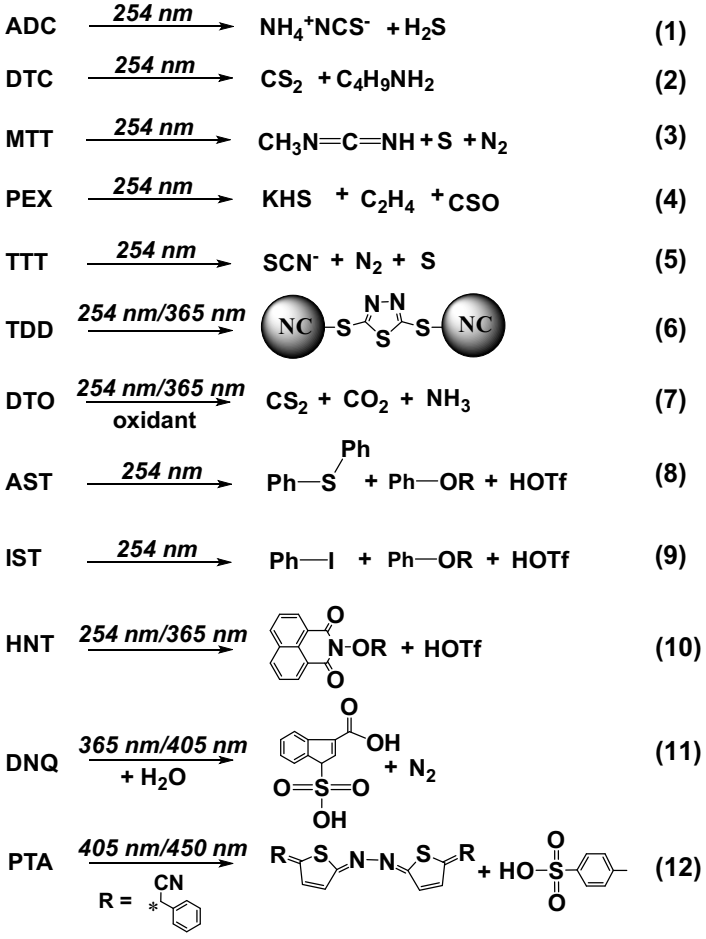

One-Component Systems

Dithiocarbamate Ligands. In this study we identify dithiocarbamate salts as a powerful platform for the development of DOLFIN ligands. To the best of our knowledge, this family has not been previously explored for photopatterning of nanomaterials. The dithiocarboxylate group can bind to surfaces of different NCs,[46-49] anchoring surface ligands responsible for colloidal stabilization in polar solvents (DMF, NMF, DMSO) as shown in Figure 1A. NCs dispersed in polar solvents such as DMF show negative zeta-potentials (Figure S1A and B) corresponding to the negative surface charge. Surface charging occurs when nucleophilic dithiocarbamate anions ($NH_2CS_2^-$ for ADC, and $BuNHCS_2^-$ for DTC) bind to uncoordinated metal atoms at the NC surface.[7,10,33,44,50-52] NH_4^+ and Na^+ cations serve as the counter-ions, forming a diffuse cloud around the NCs. During film deposition and drying, cations re-associate with their corresponding anions in order to preserve charge neutrality.

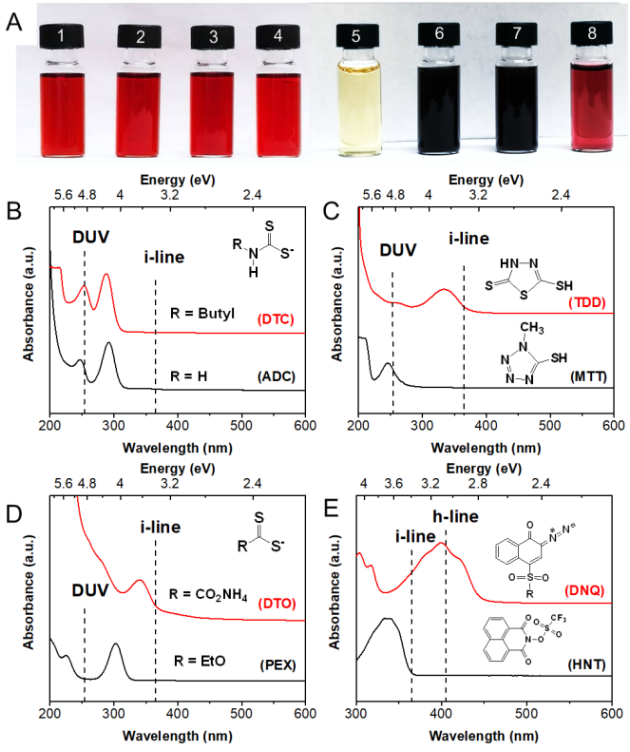

Figure 1. (A) Photographs of various nanocrystals in DMF. (1) CdSe-ADC, (2) CdSe-DTC, (3) CdSe-MTT, (4) CdSe-TDD, (5) CeO_2-DNQ, (6) CdTe-DTO, (7) CdTe-MTT, and (8) Au-PEX in DMF. (B-E) Absorption spectra of pure ligands in MeOH. (B) Ammonium dithiocarbamate (ADC, black) and butyldithiocarbamate (DTC, red). (C) 5-Mercapto-1-methyltetrazole (MTT,

black) and 1,3,4-Thiadiazole-2,5-dithiol (TDD, red). (D) Potassium ethyl xanthate (PEX, black) and ammonium 1,1-dithiooxalate (DTO, red). (E) N-hydroxynaphthalimide triflate (HNT, black) and 1,2-naphthoquinonediazide-4-sulfonyl chloride (DNQ, red).

Dithiocarbamates show pronounced UV absorption bands with spectral positions affected by substitution groups. Figure 1B shows the comparison of the absorption spectra of pure ADC and DTC ligands in MeOH. The molar extinction coefficients of these ligands at their reddest absorption peaks are $\varepsilon_{(292\ nm)} = 1.3*10^4$ M/ cm for ADC and $\varepsilon_{(287\ nm)} = 7.9*10^3$ M/cm for DTC. The absorption of ADC and DTC ligands matches reasonably well to the DUV wavelength. The photochemistry of dithiocarbamates has been extensively studied.[53-56] Depending on the substitution group, dithiocarbamate derivatives can undergo different photochemical decomposition pathways. Upon irradiation, these ligands decompose to small molecules that can serve as X-type (SCN^-, Figure S10) and L-type ($BuNH_2$, Figure S11) ligands to passivate dangling bonds and trap states at the NC surface (Scheme 3, eqs 1 and 2 and Figure S2).

Azole Ligands. Azoles are a class of five-membered heterocyclic compounds containing at least one nitrogen atom and other noncarbon atoms (*i.e.*, nitrogen, sulfur, or oxygen). For example, triazole and tetrazole derivatives containing nitrogen and sulfur atoms are used in a large number of practical applications such as pharmaceutical agents in medicine,[57] pesticides in agriculture,[58] and gas-generating agents for airbags in the automobile industry.[59] In 2008, Voitekhovich and c-workers used tetrazole derivatives to synthesize thiotetrazole capped CdS QDs.[60] Recently, Eychmuller and co-workers introduced triazoles as capping ligands to stabilize semiconductor and metal NCs using the nucleophilicity character of the azole ring.[61]

Another special property of azoles is their photolytic behavior. Maier and co-workers demonstrated that upon UV exposure, tetrazole derivatives release molecular nitrogen to form products such as nitrilimine, carbodiimide and cyanamide.[62] Further studies by Wierzejewska[63] and Rayat[64] indicated that for simple tetrazole derivatives like 5-methyltetrazole and 1-methyltetrazole, carbidiimides were the principal products, while nitrilimine, and cyanamide sometimes appeared.

Considering the aforementioned properties of azoles, we present 5-mercapto-1-methyltetrazole (MTT) and 1,3,4-Thiadiazole-2,5-dithiol (TDD) as representative examples for

the DOLFIN ligands (Figure 1A). Their photo induced decomposition pathways are shown in Scheme 3, eqs 3 and 6 (details are discussed in SI). For example, after MTT is irradiated, it decomposes into $CH_3N{=}C{=}NH$ (Figure S12), which no longer provides colloidal stability in polar solvents. In contrast, TDD undergoes a photo-induced tautomerization from a thione-thiol to a dithiol form (Figure S14), which bridges neighboring NCs, and leads to decreased solubility in polar solvents. MTT absorption is well-matches to the DUV wavelength, while TDD absorbs both DUV and i-line photons (Figure 1C). As a result, MTT-capped NCs can be patterned with DUV photons while TDD-capped NCs can be used for both DUV and i-line DOLFIN.

Xanthate and Thiooxalate Ligands. Xanthates bind strongly with transition metal cations forming charge-neutral complexes. These have been previously explored as single-source precursors for NC synthesis.[65-67] CdSe NCs capped with $EtOCS_2^-$ ligands can be easily prepared using potassium ethyl xanthate (PEX) in DMF or NMF (Figure S3) and the solutions retain excellent colloidal stability for weeks.

Another interesting ligand is thiooxalate, which is a compact, four-atom photochemically active ion (DTO in Scheme 1). Its structure enables either five-membered (side-on) or four-membered (end-on) chelate rings.[68] In the case of ammonium 1,1-dithiooxalate (DTO), the chemically soft dithiocarboxylate site ($RCSS^-$) or hard carboxylate ($RCOO^-$) can easily replace organic ligands on the NC surface.[69] We demonstrate stable colloids in DMF and NMF through a one-phase ligand exchange procedure. The generality of this approach is established for a wide range of colloidal NCs including CdSe, CdTe, CeO_2, and ZrO_2 (Figure 1A, S3 and S4). By tailoring the number of sulfur atoms, thiooxalate derivatives including monothio-oxalate, 1,2-dithio-oxalate, trithio-oxalate and tetrathio-oxalate could also serve as capping ligands in the preparation of DOLFIN inks.

Similar to dithiocarbamate and azole ligands, both xanthate and thiooxalate ligands are sensitive to UV light (Scheme 3, eqs 4 and 7, and Figure S13). As shown by their absorption spectra in Figure 1D, PEX with the absorption coefficient of $1.8*10^4$ M/cmat 302 nm [70] is sensitive to DUV light, while DTO ($\varepsilon_{(346\ nm)} = 1.5*10^4$ M/cm, in H_2O [69]) absorbs both DUV and i-line photons. We further discuss the potential decomposition pathways of each ligand that affect the solubility of corresponding NCs in polar solvents in the Supporting Information.

Two-Component Systems

In this Section we discuss NC inks containing two types of functional molecules: stabilizing ligands and photosensitive additives. Using this approach, we can achieve various special features that are not easily obtained in a single ligand. For example, the photosensitive additives allow NCs capped with non-photosensitive inorganic ligands to be patterned with 365 or 405 nm light.

Stabilizing Ligands. These may include almost any traditional organic (*e.g.*, fatty carboxylic acids and alkylamines) or inorganic (S^{2-}, $CdCl_3^-$, $Sn_2S_6^{4-}$, *etc.*) ligands, which provide colloidal stability to NCs and are not sensitive to light. In this study, we focus on two broad families: metal chalcogenide (MCC) ligands[51] and so-called "bare" NCs prepared by removing organic ligands with ligand-stripping agents.[71-73] MCC ligands such as $Sn_2S_6^{4-}$ act as negatively-charged ions that strongly bind to the NC surface while the cations form a diffuse cloud around the NC, yielding a negative zeta-potential.[50,51] Conversely, the stripping agents such as $NOBF_4$ generate "bare" NCs by removing the original long-chain organic ligands and creating a positively charged NC surface (Figure S1).[71-73] The "bare" surface contains an excess of metal cations weakly electrostatically coordinates with BF_4^- anions and DMF solvent molecules that provide colloidal stabilization of the NCs in the polar media.

Photochemically Active Additives. In contrast to stabilizing ligands, photosensitive species are designed to have minimal interactions with the NC surface when initially added to a solution. We found that these additives subsequently affect the solubility of NCs in two ways. First, the additives may serve as a physical spacer between NCs in the casted film. If the molecular size of the additive is large enough, this prevents NCs from getting too close to each other and falling into an irreversible van der Waals potential well (Figure 2). Second, the photosensitive additives decompose upon irradiation, altering the local environment around the NCs, such as local pH and ionic strength. These changes strongly impact the NC dissolution rate, making it possible to form patterns. In this work, we investigated two types of additives, ionic and nonionic photoacid generators (PAGs).[74]

Well-known classes of ionic PAG are the aryl sulfonium triflate (AST) and aryl iodonium triflate (AIT) ionic salts, which release triflic acid upon DUV irradiation (Scheme 3, eqs 8 and

9).[75] By adjusting the conjugated π-system of the cation, one can extend the absorption band to about 360 nm.[76] The advantages of these compounds are their good thermal stability and high solubility in polar solvents, which allow for high loadings of PAG in the NC films. The role of the bulky PAG cation as a spacer is evident when compared with triflic salts of smaller cations: a CeO_2 NC film containing AST easily redissolves in DMF after vacuum drying (without UV exposure), while the films of same NCs with sodium or silver triflate salts do not (Figure S5). Small-angle X-ray scattering measurements on films with added PAG also show a relatively large increase in NC spacing (~ 1 nm) compared to films without PAG additives (Figure S6). Subsequent UV irradiation of the PAG cleaves a Ph-S bond and forms reactive protons that interact with either the surface ligands or NC surface, rendering particles insoluble in DMF.

Another ionic PAG utilized is 1,2-naphthoquinonediazide-4-sulfonyl chloride (DNQ), which has a broad absorption band spanning 340 – 450 nm.[77] Dissolving DNQ in nonanhydrous DMF allows DNQ to hydrolyze with ambient water vapor to form the corresponding sulfonic acid. With the assistance of irradiation (365 nm or 405 nm light), DNQ molecules further produce a carboxylic acid moiety with the release of N_2 (Scheme 3, eq. 11, Figure 1E and 6A).[78] These two binding sites (sulfonate and carboxylate) can attach to neighboring NCs, thereby reducing the NC dissolution rate during development. It is of interest to note that moving the 4-sulfonyl group to the 5- or 6- position will further red-shift the wavelength sensitivity up to 500 nm.[79]

Non-ionic PAGs are neutral organic molecules containing functional groups such as carbonic esters, chloromethyl triazines, imino sulfonates, N-hydroxyimide sulfonates, *etc*.[74,80] The diversity in chemical structures allows the photosensitivity to be tuned across a wider range of wavelengths. Like ionic PAGs, the non-ionic PAGs can also function as photosensitive additives that turn NC solutions into DOLFIN inks. For example, HNT is sensitive to 365 nm light and liberates triflic acid by cleaving the N-O bond (Scheme 3, eq. 10, and Figure 1E).[74] By simply mixing HNT with "bare" CeO_2 NCs, the resulting ink can be directly implemented in the DOLFIN process. We attribute the patterning mechanism to changes in local ionic concentration, which compresses the electrostatic double layer around the NCs, reducing repulsion between NCs and resulting in a slower dissolution rate.[81]

The step-by-step changes during the DOLFIN process using non-ionic PAGs are outlined in Figure 2, which uses numerically calculated DLVO interaction energy (details provided in the Supporting Information and Figure S27). In a solution of CeO_2 NCs and HNT, the electrostatic

double layer repulsion dominates, which prevents particle aggregation (Figure 2, (1)). In the film-formation step, the solvent evaporates, forcing the particles to approach each other and settle into a randomly-packed structure with surface-to-surface separation equaling the size of the PAG (Figure 2, step 1→2a). Upon UV irradiation, the local ionic concentration in the film increases significantly which reduces the electrostatic repulsion between NCs, leading to the removal of the barrier in the interparticle interaction energy (Figure 2, step 2a→2b). This allows NCs to come much closer together, sinking into a deep potential well and becoming insoluble during development (Figure 2, step 2b→3b). On the other hand, the regions of NC film that were *not* exposed to UV light reestablish the double layer repulsion during the development step, allowing NCs to easily separate from one another and dissolve into the developing solvent (Figure 2, step 2a→3a). An alternative mechanism for nonionic PAG lithography of NCs was recently proposed.[40] The triflate ion (from HNT decomposition) was hypothesized to act as a stronger binding ligand that displaces the original weakly associated ligands at the NC surface, leading to a difference in solubility between the exposed/unexposed area. However, we found that triflate-stabilized NCs can also be directly patterned with triflate based PAG additives (HNT) under comparable conditions (Figure S28). This indicates that the photo-induced ligand exchange, if observed, is most likely a secondary effect during the patterning process.

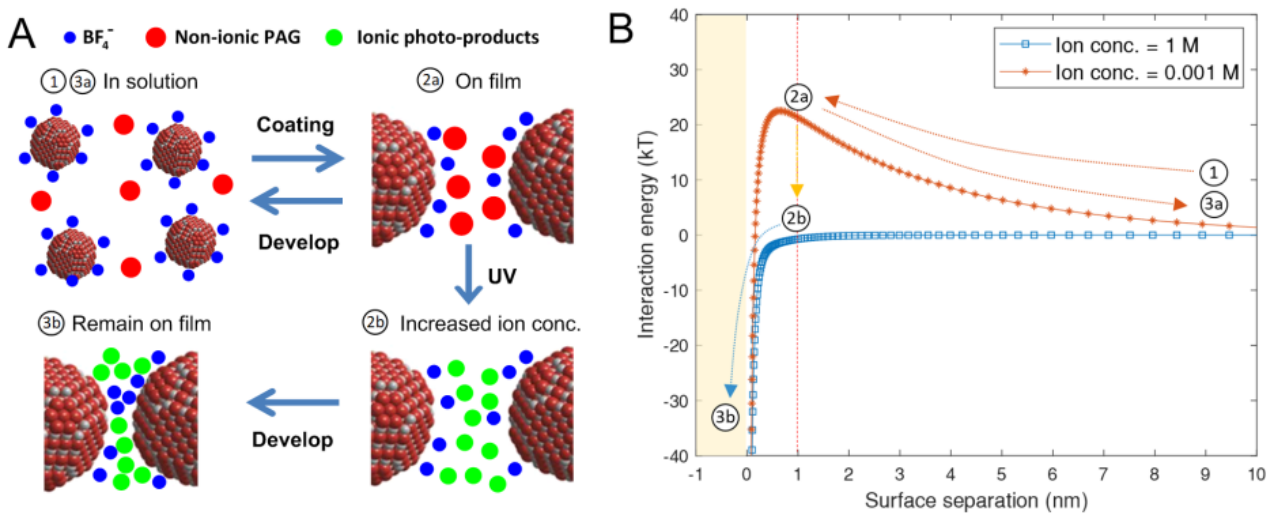

Figure 2. (A) Schematic of non-ionic PAG DOLFIN (B) Numerically calculated interaction energy (DLVO) curves for 1.3 nm CeO_2 NCs in solutions of two different ionic concentrations; low concentration (0.001 M) represents the condition of NC inks before irradiation; high concentration (1 M) represents the condition of NC inks after irradiation (further details provided in Figure S27).

Lithography: DOLFIN Patterning of Colloidal NCs

As we discussed above, the ligands used for NC inks show different absorption spectra, spanning different regions in the UV- visible range (200 nm to 450 nm, Figure 1B-E). According to their optical properties, these ligands can be divided into four groups: solely sensitive to DUV light (ADC, DTC, MTT and PEX), sensitive to both DUV and i-line (365 nm) photons (DTO, TDD and HNT), sensitive to both i-line and h-line (DNQ) and sensitive to both h-line and visible light (PTA). Most of the above ligands are compatible with CdSe NCs and are typically compatible with other semiconductor NCs (CdTe, CdSe/ZnS, InP/ZnS), oxide NCs (CeO_2 and ZrO_2) and metal NCs (Au), as shown in Figures 1A, S3, and S4. The NCs capped with photoactive surface ligands preserved their morphology and electronic structure which was confirmed by UV-Vis (Figures 3A, C, E and S7), TEM (Figure S8), powder X-ray diffraction and FT-IR (Figure S9) measurements. Table 1 summarizes the explored NC-ligand combinations and basic patterning conditions, such as deposition and developer solvents, exposure wavelength and dose.

Table 1. Tested NC-ligand combinations and patterning conditions.

Ligand	Materials	Solvents	Developers	Dose (mJ/cm^2)
ADC	CdSe, CdTe, CdSe/CdS, CdSe/ZnS, InP/ZnS	DMF, NMF	DMF NMF	100 (254 nm)
DTC	CdSe, CdTe, FePt, HgTe	DMF, NMF	Acetone, DMF	150-180 (254 nm)
MTT	CdSe, CdTe	DMF, NMF	DMF	100 (254 nm)
PEX	CdSe, CdTe, Au	DMF, NMF	DMF	31.5 (254 nm)
TDD	CdSe, CdTe, CdSe/CdS, CdSe/ZnS, InP/ZnS	DMF	NMF	100-150 (254 nm) 80-100 (365 nm)
DTO	CdSe, CdTe, CeO_2 ZrO_2	DMF, NMF	NMF	100 (254 nm) 225 (365 nm)
HNT	CeO_2, ZrO_2, FePt	DMF, NMF	DMF, NMF	80 (254 nm) 600 (356 nm)

DNQ	CdSe, CeO_2, ZrO_2	DMF	DMF TMAH	400 (365 nm) 400 (405 nm)
PTA	CdSe, CdTe	DMF	NMF	300 (450 nm)

DOLFIN with DUV Photons (254 nm). In ref. [33] we introduced TTT and AST/IST molecules as two ligand systems for NC patterning using 254 nm photons. In this current study, we expanded the choice of ligands and added ADC, DTC, MTT and PEX ligands sensitive exclusively to 254 nm photons. These ligands bind to NC surfaces without affecting the excitonic absorption features of the NCs (Figures 3A, C, E and S5). Figures 3B, D, F and S15A show top view SEM and optical images of CdSe NC layers patterned using various photoactive ligands. The cross-section SEM image in Figure S15C indicates that the thickness of a patterned CdSe NCs layer is around 100 nm which is in agreement with a prior estimation.[33] It is worth noting that the quality of each pattern is slightly different although the starting NCs are the same. This indicates that the resolution and sensitivity of the inks are determined by the photosensitive surface ligands and should be optimized for each case. As shown in Figure 3D, the smallest feature resolved is ~1 μm using the MTT capped NCs with an exposure dose of 100 mJ cm^{-2}, while PEX-CdSe NCs showed the highest sensitivity, with a clear contrast developed after DUV illumination with a 31.5 mJ cm^{-2} exposure dose, which is much lower than what is used for other DOLFIN ligands (Table 1). In Figure S26, we show that a layer of Au NCs patterned using PEX ligands and then annealed at 150 °C for 20 min exhibited very high conductivity.

For the DTC ligand, acetone can be used both as a solvent and developer (Figure S15B). Since acetone is a more widely industrially used solvent, this feature can be beneficial for the process scale up.[82] The advantage of ADC-based NC ink is pronounced when the ligand is introduced to treat CdSe/CdS core-shell NCs, which preserves bright emission (PLQY = 48%) in DMF and other polar solvents (Figure S4). From the Fig S29 A and B, we observed that the PLQY was dropped by almost 40% after ADC treatment. For comparison with the previous studies of ligand-exchanged QDs, the decrease of PLQY for QDs using MCC-type ligands such as $Sn_2S_6^{4-}$ capped core-shell NCs was 55-70%,[50] and in thiolated amino PEG capped core-shell QDs was 60-70%.[83]

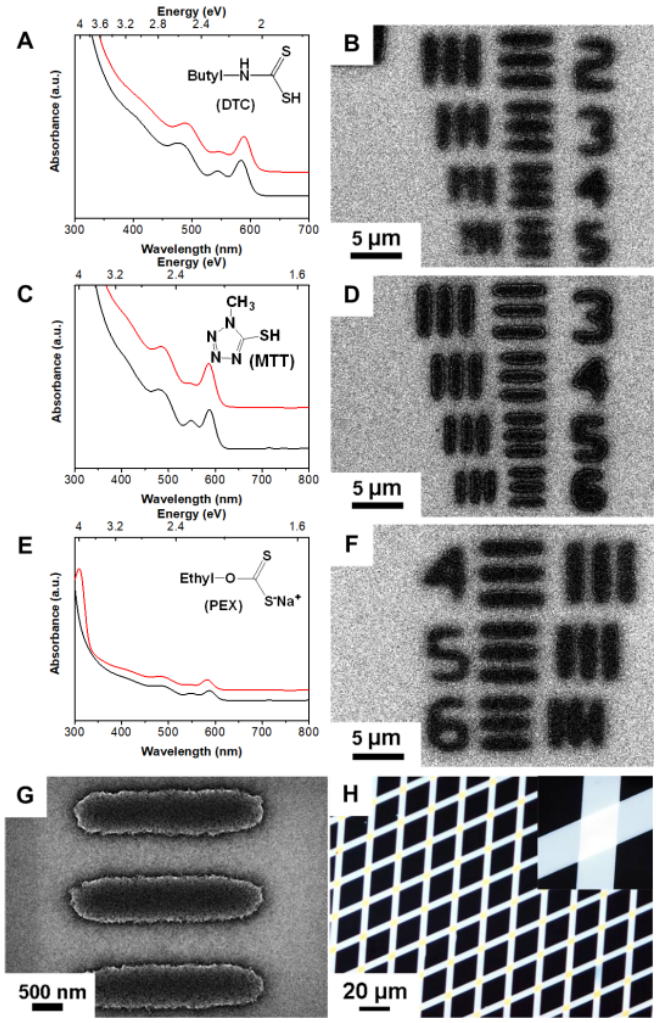

Figure 3. Examples of NCs patterned with 254 nm (DUV) exposure. Absorption spectra of Wz-CdSe NCs before (black) and after (red) capping with inorganic ligands in DMF (A) DTC, (C) MTT, and (E) PEX. SEM image of patterned USAF resolution test grids with CdSe-DTC NCs (B), CdSe-MTT NCs (D), CdSe-PEX NCs (F). (G) SEM image of patterned USAF resolution test grids with "bare" CeO_2 NCs with (p-CH_3S-C_6H_4)(C_6H_5)(CH_3)S^+OTf^- DOLFIN inks. (H) Optical microscopy images of two sequentially patterned "bare" CeO_2 NC layers with 5-µm-wide stripes using the same ink as in (G).

In addition to the single-ligand system, sulfonium triflate can be used as a photoactive additive to "bare" oxide NCs. The quality of patterns, as in the case of "bare" CeO_2 NCs with (p-CH_3S-C_6H_4)(C_6H_5)(CH_3)S^+OTf^- PAGs (5 wt%), were evaluated by the resolution, sensitivity and line edge roughness (LER). We used a 1951 U.S. Air Force target to estimate the smallest features that can be resolved. The SEM image in Figure 3G demonstrates the high contrast

features obtained from the CeO_2 ink with a resolution below 700 nm at a 100 mJ cm^{-2} exposure dose. The pattern sensitivity is similar to that of TTT inks (80-150 mJ cm^{-2}), but the resolution is comparatively higher (~1 μm for TTT ink).[33] The LER was determined from the SEM image in Figure S16, in which the edges of patterned regions are sharp and clean with roughness below 50 nm. We demonstrated the good fidelity, another parameter to verify the quality of patterns, by patterning 5 μm wide CeO_2 NC stripes consecutively on top of each other (Figure 3H).

The above examples demonstrate a wide selection of DOLFIN ligands sensitive to DUV photons. Depending on a particular application, it should be possible to identify optimal NC-ligand combinations within general constraints (*e.g.*, small penetration depth) imposed by the fundamental nature of DUV photons.

Patterning with i-line (365 nm) Photons. The previous DOLFIN methods used ligands sensitive to only DUV light.[33,84] However, lower energy photons (*e.g.* 365 nm, 405 nm and 450 nm) generally create less sample damage (*e.g.* oxidation, sintering, *etc.*), and enable deeper light penetration into the patterned layers.[34,35] In addition, significantly less expensive infrastructure is required to generate and focus 365 nm and visible light. These benefits come at the expense of the ultimate resolution determined by the Abbe diffraction limit, which is not the limiting factor for many practical applications, such as patterning LED pixels, optical gratings or photodetector arrays.

Here we show that DTO and TDD ligands along with HNT, a non-ionic PAG additive, enable patterning of 1 μm-spaced features using 365 nm light (Figure 4D-G). As shown in Figures 4A and S7, TDD and DTO ligands do not change the electronic structure of CdSe NCs. The exposure dose required for pattern development varies depending on the ligands: 80-100 mJ/cm^2 for TDD, and ~225 mJ/cm^2 for DTO. The same ligands can also be used for 254 nm patterning. For example, we obtained a DTO capped CdSe NC patterns with comparable resolution with an exposure dose of 100 mJ/cm^2 (Figure S17).

One of the advantages of DTO ligands over other photosensitive small-molecule ligands is the clean photodecomposition pathway (Scheme 3, eq. 6). Upon exposure to UV light, DTO ligands photolytically decompose to CS_2, CO_2 and NH_3 gases (Scheme 2).[69] As a result, almost no molecular byproducts remain in the film after the photopatterning step which was confirmed by FT-IR (Figure S18). The second benefit of the DTO ligand is its versatility as a capping agent.

For example, the DTO ligand can be used to stabilize both chalcogenide (CdS, CdTe, *etc*.) and oxide NCs, such as CeO_2 and ZrO_2 NCs (Figure 1A, S3 and S4). Similar solubility changes are also observed when the DTO capped oxide NC inks are exposed to 365 nm UV light. The smallest features (~1 μm) are successfully obtained from CeO_2-DTO NCs inks with a 225 mJ/cm^2 exposure dose (Figure 4F).

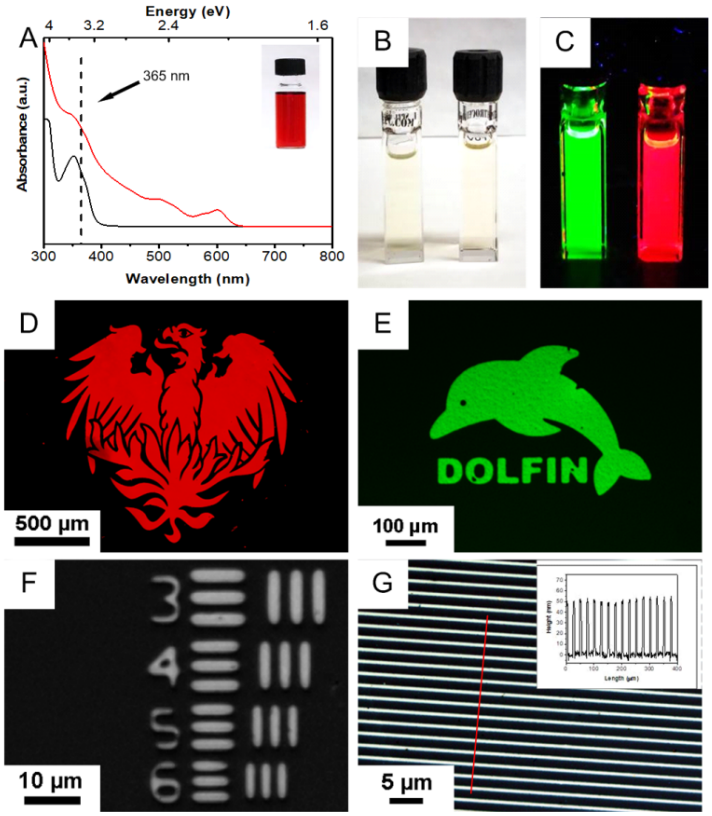

Figure 4. DOLFIN patterning with 365 nm photons. (A) Absorption spectra of inorganic ligands TDD in MeOH (black) and Wz-CdSe NCs capped with TDD in DMF (red). Photographs of colloidal solution of red-emitting CdSe/ZnS and green-emitting InP/ZnS NCs capped with TDD ligand in DMF under ambient light (B) and UV light (C). Optical microscopy images of various NCs patterned with 365 nm UV light: (D) CdSe/ZnS-TDD NCs, (E) InP-ZnS-TDD NCs, (F) CeO_2-DTO NCs, and (G) ZrO_2 NCs with HNT. The University of Chicago Phoenix in panel (D) is reproduced with permission from UChicago Creative.

TDD is another ligand that can be successfully applied to prepare DOLFIN ink for i-line lithography (Figure 4B). Similar to ADC, the advantage of TDD based NCs ink is pronounced when the ligand is introduced to pattern luminescent core-shell NCs. The core-shell CdSe/ZnS NCs stabilized by TDD preserve bright emission in polar solvents (Figure 4C, Figure S29C and D). We can pattern brightly luminescent red InP/ZnS and green CdSe/ZnS NCs with the dose of 80-100 mJ/cm^2 as shown in Figures 4D and 4E.

Patterning with i-line photons can be also implemented using a two-component system. For example, "bare" CeO_2 NCs electrostatically stabilized with BF_4 ions and DMF can be patterned with the assistance of HNT, a typical non-ionic PAG sensitive to 365 nm photons (Figure 4G), following the mechanism described in Figure 2. The patterned features demonstrate efficiently resolved sub-micron lines (Figure S19A), which is comparable to the resolution of NC patterns we achieved with DUV lithography. However, with the same concentration of PAG in the ink (2.5 wt %), the required dose for patterning with 365 nm light was 500-600 mJ/cm^2, larger than that required for DUV patterns. This is because the absorption coefficient of HNT at 365 nm was four times smaller than that at 254 nm (Figure S19B), and the overall acid releasing efficient was smaller, which in turn lowered the sensitivity of NCs inks.

The two-component system provides us with a powerful tool for device integration of functional NCs. As a proof of concept, here we demonstrate optical diffraction gratings using solution-processed NC films composed of high-refractive-index oxides patterned with 365 nm photons. Such diffraction gratings are actively used in spectroscopy,[85] optical biosensors[86] and structural coloration.[87] A periodic pattern of diffraction grating which creates a diffraction image in the far field, with bright diffraction orders given by the equation $d \sin\theta = m\lambda$, where d is the grating pattern spacing, θ is the diffraction angle and $m = 0, \pm1, \pm2$, *etc* (Figure 5A).

Our binary phase diffraction grating prototypes are fully transparent and consist of periodic patterns of a high refractive index material on a glass substrate. They are fabricated in one or two DOLFIN steps (Figures 5B and 5C). Organic ligands capped CeO_2 NCs are first converted into DOLFIN ink by mixing bare NC inks with HNT as described above, then 5 μm-wide, ~100 nm-thick CeO_2 NC stripes with a 25 μm period are patterned on a glass substrate to form 1D grating (Figure 5B). Two consecutive, orthogonal periodic oxide patterns form a 2D grating (Figure 5C). These gratings have good optical transparency with no visible haze. Many high order diffraction maxima are formed upon irradiation with a red (Figures 5D and 5G), green (Figures 5E and 5H)

or blue (Figures 5F and 5I) continuous wave (CW) laser. Naturally, these all-inorganic diffraction gratings have excellent thermal stability (tested up to 600 °C) and high optical damage threshold. Further studies are being carried out to fabricate gratings with smaller periods, thicker films and higher refractive index NCs. Nevertheless, we believe that the modularity and simplicity of the DOLFIN process has a clear advantage over traditional fabrication techniques, which require multiple resist coating, exposure, deposition/etching and lift-off steps.

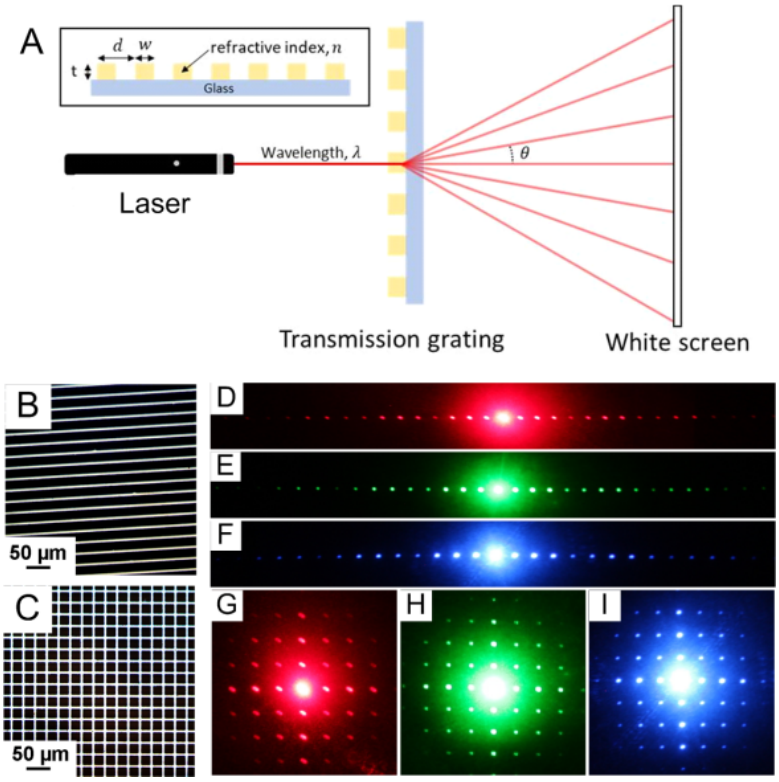

Figure 5. (A) Diffraction grating scheme (Note: figures not drawn to scale). ((B) Optical microscopy images of CeO_2 NCs in a 1D pattern. (D-F) Diffraction patterns obtained by illuminating 1D grating patterns with red, green and blue CW laser. (C) Optical microscopy images of CeO_2 NCs in a 2D pattern. (G-I) Diffraction patterns obtained by illuminating 2D grating patterns with red, green and blue CW lasers.

Patterning with h-line (405 nm) and visible (450 nm) photons. It is challenging to find a small molecule that can both colloidally stabilize NCs and be photosensitive to h-line or g-line photons. The two-component systems look most promising because of their chemical flexibility. We

prepared various NC inks by tuning the combination of inorganic ligands and photosensitive molecules. Here, we use 1,2-naphthoquinonediazide-4-sulfonyl chloride (DNQ) as an example of photosensitive molecules to prepare NC inks for DOLFIN patterning with 405 nm light (Figure 6A) and 2-phenyl-2-(-5-((tosyloxy)imino) thiophen-2-ylidene)acetonitrile (PTA) as an example of photosensitive molecules to prepare NC inks for DOLFIN patterning with 450 nm light (Figure 7A).

Both DNQ and PTA molecules function as additives in the two-component DOLFIN inks, thus they can be directly added into solution containing NCs with either positively ("bare" NCs) or negatively charged (NCs capped with inorganic ligands) surfaces (Figures S3 and S20). Figure 6B compares the absorption spectra of CdSe-Sn_2S_6 NCs before and after they were mixed with DNQ. The first excitonic peak shows almost no changes indicating the CdSe NCs retain their mean size and monodispersity. Positive-tone patterns can be obtained by using DNQ based "bare" CeO_2 NC ink and $Sn_2S_6^{4-}$ capped CdSe NCs ink with optimized developing solvents described in the Experimental Section (Figures 6C and 6D respectively). For example, DMF was used to develop the oxide NCs films, while 0.05 M tetramethylammonium hydroxide (TMAH) aqueous solution was used to develop the semiconductor NC films. Both systems produce 1.5 µm line-space features (1.5 µm lines with 1.5 µm spacings), which was the smallest feature on our mask. A typical exposure dose is around 400 mJ/cm^2.

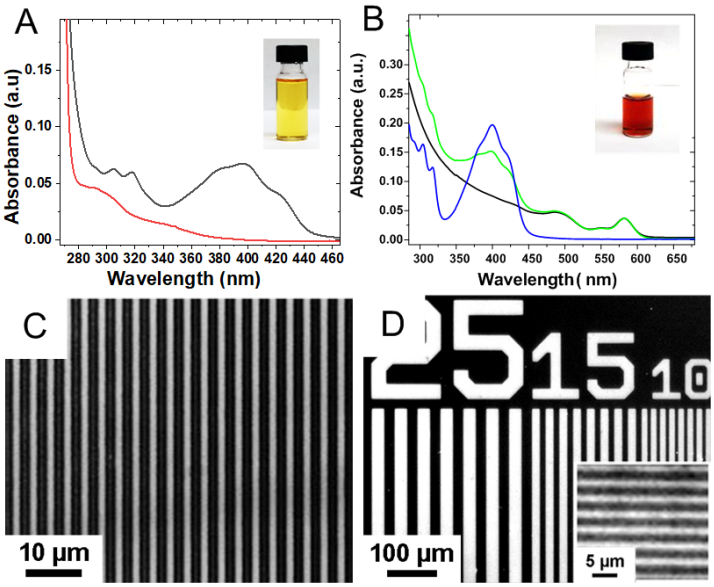

Figure 6. DOLFIN patterning with 405 nm photons. Absorption spectra of (A) DNQ ligands in DMF before (black) and after photodecomposition (red), and (B) Wz-CdSe- Sn_2S_6 NCs before (black) and after (green) mixing with DNQ. Inset: (A) DNQ salts and (B) DNQ based CdSe-Sn_2S_6 NCs ink in DMF. Optical microscopy images of equal spacing strips patterns obtained from DNQ based "bare" CeO_2 NCs ink (C) and CdSe-Sn_2S_6 NCs ink (D) using 405 nm photons.

PTA molecules are synthesized based on previous work and described in the Experimental Section. The preparation of NC inks with PTA is carried out in a similar manner with that of DNQ inks. Typically, a 450 nm photon sensitive ink is prepared by mixing PTA molecules with CdSe-Sn_2S_6 NCs in a concentration of 5 % by weight in DMF. The NCs in the photosensitive ink retain their electronic structure and size distribution, as evidenced by the excitation features in the absorption spectra shown in Figure 7B. With the exposure dose of 300 mJ/cm^2, positive-tone patterns of CdSe-Sn_2S_6 NCs can be obtained by using NMF as a developing solvent (Figure 7C). With some optimization, 2.5 μm line-space features can be easily achieved as shown in Figure 7D.

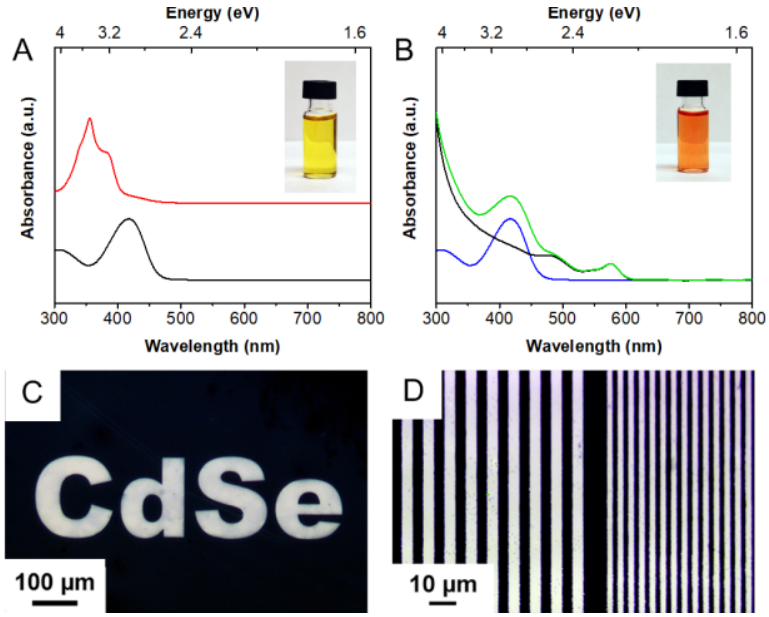

Figure 7. DOLFIN patterning with 450 nm photons. Absorption spectra of (A) PTA ligands in DMF before (black) and after photodecomposition (red), and (B) Wz-CdSe- Sn_2S_6 NCs before (black) and after (green) mixing with PTA. Inset: (A) PTA salts and (B) PTA based CdSe-Sn_2S_6 NCs ink in DMF. Optical microscopy images of patterns obtained from PTA based CdSe-Sn_2S_6 NCs ink (C and D) using 450 nm photons.

Direct Electron Beam Lithography of Functional Inorganic Nanomaterials (DELFIN). Electron beam lithography (EBL) is a powerful technique that uses a focused electron beam for direct-write patterning with very high resolution. EBL enables much better resolution compared to traditional photolithography because the electron beam has an extremely short wavelength (0.2-0.5 Å) and can be focused down to the sub-nanometer scale.[88] Hence, the resolution is not determined by the diffraction limit,[89,90] enabling very small features.[91] Three different approaches were previously used to pattern NCs with EBL: (i) a polymer e-beam resist was used as a mask for subsequent inorganic materials deposition,[92] (ii) NCs were blended with a polymer e-beam resist into hybrid organic-inorganic composites,[84] and (iii) NCs were stabilized by organic ligands that crosslinked under e-beam.[93] Here, we demonstrate direct e-beam lithography of functional inorganic nanomaterials (DELFIN), which enables direct patterning of nanomaterials with sub-100 nm resolution without diluting NC with organic resists and other impurities that block charge and heat transport through the patterned layers. Similar to DOLFIN, the DELFIN process uses e-beam sensitive NC inks. Because many PAGs are sensitive to the e-beam exposure,[94] we explored PAG-type positive-tone DOLFIN inks for e-beam patterning.

In DELFIN, PAG molecules release a strong acid through the electron-beam-induced radical reaction that occurs upon e-beam exposure.(Eq. S1).[88] The protons subsequently bind with either NC ligands or Lewis-basic sites at the NC surface,[33] resulting in the loss of colloidal stability. When soaked in polar solvents like DMF or NMF, the unexposed areas readily redissolved while the exposed regions remained insoluble generating a positive pattern. The unreacted PAG molecules as well as the reaction byproducts from PAGs were removed during the solvent development step.

Figures 8A and 8B show SEM images of patterned CeO_2 NCs with well resolved 50 nm and 30 nm pattern dimensions obtained under the same e-beam current of 17.6 pA, but various doses, from 150 to 200 $\mu C/cm^2$. Larger patterned features, 300 nm and 100 nm can be obtained with 80 $\mu C/cm^2$ and 100 $\mu C/cm^2$ doses, respectively (Figures S21A and S21B). It is interesting to note that patterning smaller features requires a higher dose, which may be due to the fact that the high dose can effectively avoid the blur during exposure.[41,95] This electron dose is comparable to the doses used for patterning organic e-beam resists.[96] Considering the NC size of 2 nm determined by dynamic light scattering (Figure S22A), and the film thickness of 50 nm measured by a

confocal optical surface metrology microscope (Figures S22B and S22C), the highest resolution DELFIN feature consists of a stack of about 15 NCs in width and at least 25 NCs in height. The LER is around 5 nm which equals to the size of two single NPs (Figure S21C). The clean background and sharp pattern edge observed in the enlarged SEM images in Figure 8 demonstrate high resolution capabilities of the inorganic inks achieved with significantly high sensitivity.

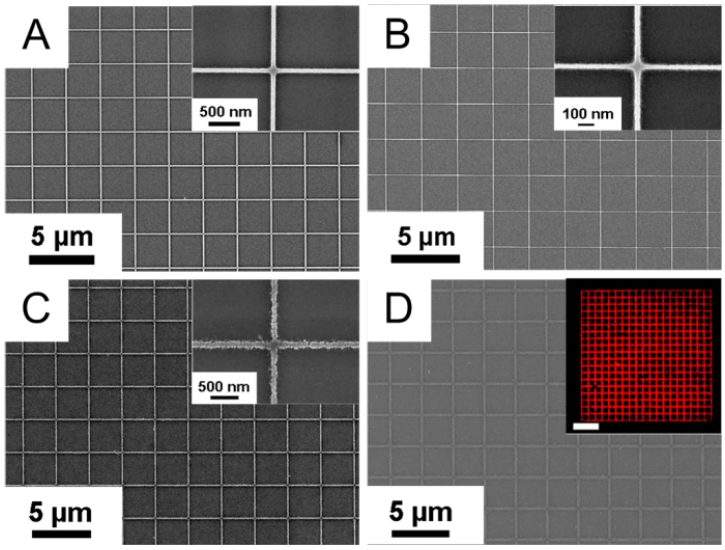

Figure 8. Direct e-beam lithography of functional inorganic nanomaterials (DELFIN). SEM image of EBL-patterned "bare"CeO_2 with a line width of (A) 50 nm, and (B) 30nm. (C) CdSe-Sn_2S_6 NCs patterned with a line width of 100 nm and (D) CdSe/ZnS-Sn_2S_6-PAG with a line width of 100 nm. The inset shows photoluminescence from 100 nm wide stripes of CdSe/ZnS NCs, patterned with e-beam, scale bar: 10 µm.

Besides oxide NCs, semiconductor QDs can be patterned by the DELFIN process. For example, Figure 8C shows 100 nm wide lines obtained from the inks of CdSe NCs capped with $Sn_2S_6^{4-}$ ligands and Ph_3S^+ PAG counter ions using an e-beam with a dose of 80-100 µC/cm^2. The ultimate resolution evaluated from SEM images is about 70 nm, which is a record small all-inorganic semiconductor feature from direct EBL (Figure S23).[41,95] Because the size of CdSe NCs is around 5 nm (Figure S24A) and the thickness of the film is around 40 nm (Figures S24B and S24C), the smallest features of CdSe NCs achieved by DELFIN is a line of about 14 NCs in width and 8 NCs in height. Importantly, under the same E-beam exposure conditions, we demonstrated 100 nm line patterns of CdSe/ZnS core-shell QDs (Figure 8D). After developing in

NMF, such small features still showed bright photoluminescence, which indicate that DELFIN can be used to fabrication of various QD nanodevices.

Conclusions

We have designed a series of photo- and electron beam sensitive ligands, thus building an extensive library of functional photosensitive inorganic inks. With these designed ligands, we are able to directly pattern a variety of technologically important materials using not only DUV light, but also 365 nm i-line UV light, 405 nm h-line blue light and 450 nm visible light. The DOLFIN inks show a potential application for other patterning techniques besides photolithography. By taking the advantages of electron beam, much higher resolution is achieved with DELFIN. These strategies will help us further develop DOLFIN and DELFIN methods as a powerful and versatile nanomanufacturing platform that complements traditional photopolymer lithography and expands our current nanomanufacturing capabilities.

Experimental Section

Synthesis of Colloidal NCs and Photosensitive Ligands. Detailed synthetic protocols are provided in the SI.

Preparation of Photochemically Active Inks. All preparation processes were carried out in ambient conditions or in a glovebox (for sensitive materials) equipped with a yellow filter typically used for clean room lighting, purchased from Pro Lighting Group, Inc. We typically used anhydrous solvents and a one-phase ligand exchange strategy to treat the NC surface. In a typical one-phase ligand exchange approach, the solvent in the NC dispersion was the same as that of inorganic ligands, such as acetone, or formed a homogeneous mixture with the solvent used for inorganic ligands, such as toluene/DMF or toluene/NMF. Therefore, the NC and ligand solutions were miscible when mixed and surface ligand exchange was achieved in one phase.

NC with Photosensitive Ligands:

NCs Capped with ADC and TDD Ligands. Both ligands were used to prepare the QD inks with bright luminescence. For example, 100 μL of core-shell CdSe/ZnS NCs (40 mg/mL) was diluted

into 1 mL of toluene forming a colloidal solution, into which 100 μL of ADC (0.5 M) or TDD DMF solution (0.25 M) was added. A flocculation was observed after vortexing for several minutes, indicating a dramatic change in NC solubility caused by the surface modification. The ligand-exchanged CdSe/ZnS NCs were precipitated from the suspension by centrifugation and purified by dissolution–precipitation procedure with DMF and toluene two times. After purification, the NCs were redissolved in 100 μL of DMF as a colloidal solution with a concentration of 30-40 mg/mL and stored in the dark in a glovebox, which kept them stable for weeks.

NCs Capped with DTC Ligands. Using CdSe NCs (4.5 nm, wurtzite phase) as an example, 100 μL of the as-synthesized NCs (40 mg/mL) were precipitated first from toluene by adding 1.5 mL of acetone, and were then re-dispersed into 0.5 mL of acetone forming a cloudy suspension. After adding 200 μL of fresh DTC solution in acetone (0.2 M) and vortexing for 1 min, the cloudy NCs suspension turned into red colloidal solution. The treated NCs were then precipitated by adding 2 mL of MeOH and rinsed with MeOH to remove free DTC ligands. After purification, the CdSe-DTC NCs were redissolved into 100 μL of DMF as a colloidal solution with a concentration of 30-40 mg/mL.

NCs Capped with DTO, MTT and PEX Ligands. The surface treatment process was similar for preparing of photosensitive inks with DTO, MTT or PEX ligands. In general, photosensitive ligands were dissolved into N-methylformamide (NMF) or N,N-dimethylformamide (DMF) forming a stable solution with a concentration of 0.2 M. In a separate vial, 100 μL of the as-synthesized NCs (40 mg/mL) were diluted with 1 mL of toluene. After introducing 200 μL of ligands solution and vortexing, the colloidal NCs solution became cloudy. The treated NCs were washed with toluene and MeOH, and finally redissolved into 100 μL of DMF to form a solution with a concentration of 30-40 mg/mL.

Two-Component Photosensitive NC Inks:

Bare NCs with PAG Ligands. To prepare starting materials, we treated NCs with $NOBF_4$ to obtain ligand-free bare NCs following the approach of Murray *et al*.[7171] For example, CeO_2 NCs capped with organic ligands were diluted with toluene to form a stable solution with a concentration of 80 mg/mL. $NOBF_4$ used as a ligand stripping agent was first dissolved in DMF (20 mg/mL) and then introduced into the CeO_2 NC solution with the amount of 2:1 (NCs:

$NOBF_4$) by weight. The precipitate was isolated by centrifugation and washed with toluene at least three times. The resulting CeO_2 NCs were purified using toluene and DMF for several precipitation–redispersion cycles. Purified NCs were dissolved in DMF at a concentration of ~40 mg/mL. The photosensitive ink was then prepared by mixing these CeO_2 NC colloids with different amounts of photosensitive molecules (2.5wt % for DOLFIN and 15% for DELFIN) in a DMF and MeOH co-solvent system (v/v: 10:1). For different inks, such molecules could be (*p*-CH_3S-C_6H_4)(C_6H_5)$_2S^+OTf^-$ (for DUV and DELFIN), N-hydroxynaphthalimide triflate (HNT, for i-line patterning and DELFIN), and diazonaphthoquinone (for h-line patterning).

Direct Patterning of Inorganic Materials.

The experiments were performed under yellow light and photoactive inorganic inks were passed through a 0.2 μm filter before spin-coating to eliminate particulate contaminations. In this work we used DOLFIN to obtain the patterns with submicron resolution, and DELFIN to obtain features with sub-100 nm resolution.

In a general DOFLIN procedure, the aforementioned photosensitive colloidal solutions were prepared in DMF with a concentration of about 30 mg/mL and spin-coated (spread: 400 rpm, 10 s; spin: 2000 rpm, 60 s) on various substrates (Si/SiO_2, Si, quartz, glass). The NC layers were then irradiated with either a 254-nm DUV lamp, a 365 nm i-line light, a blue 405 nm h-line light or a 450 nm visible light through a chrome mask held together in a Mask Aligner system or using binder clips. The exposure dose and developer solvents varied, depending on the ligands. Typical parameters are listed in Table 1. Taking CdSe-DTC inks as an example, both DMF and acetone could be used to form NC ink. In order to obtain the NC layer from acetone with the same thickness as that from DMF solution, the concentration of NCs in acetone should be decreases to 10-15 mg/mL, due to the its higher volatility. A dose of 150-180 mJ/cm^2 was required for DUV lithography and 150 mJ/cm^2 was needed for 365 nm i-line patterning. Both neat DMF and acetone could be used as developer solvents in this case. A 1951 USAF target, one of the most frequently used standard resolution tests, was introduced in our work to determine the pattern resolutions. This target assembles numbered elements and groups with precisely defined space, the limiting resolution can be measured by determining the smallest features, both vertically and horizontally.

Associated Content

The authors declare no competing financial interests.

Supporting Information

The Supporting Information is available free of charge on the ACS Publications website at DOI.XXXXX

Experimental details of NCs synthesis and photosensive ligands preparation; Photographs of various DOLFIN inks and NC films; Zeta potential measurements of NCs capped with photosensive ligands; Absorption spectra of photosensitive NC inks; TEM image, FTIR spectra and XRD patterns of functional NCs; Small-angle X-ray scattering measurements of "bare" CeO_2 NCs with PAG additives before and after UV exposure; SEM images and optical microscopy images of patterned NCs; Decomposition pathway studies of photosensitive ligands; Refractive index study of patterned CeO_2 NCs; and conductivity measurements for solution-processed Au NC patterns. (PDF)

Author Information

Corresponding Author

dvtalapin@uchicago.edu

Author Contribution

§ These authors contributed equally to this work.

Acknowledgments

We would like to thank V. Kamysbayev for help with SAXS measurements and T. Shpigel for reading the manuscript. This work was supported by the Department of Defense (DOD) Air Force Office of Scientific Research under grant number FA9550-18-1-0099 and NSF under award number CHE-1905290. J.-A.P. was supported by the University of Chicago Materials Research Science and Engineering Center funded by NSF under award DMR-1420709. D.V.T. acknowledges support from Samsung Global Research Outreach Program on New Materials. Use of the Center for Nanoscale Materials, an Office of Science User Facilities operated for the U.S.

Department of Energy (DOE) Office of Science by Argonne National Laboratory, was supported by the U.S. DOE under Contract No. DE-AC02-06CH11357.

References

1. Alivisatos, A. P., Semiconductor Clusters, Nanocrystals, and Quantum Dots. *Science* **1996,** *271*, 933-937.

2. Dabbousi, B. O.; Rodriguez-Viejo, J.; Mikulec, F. V.; Heine, J. R.; Mattoussi, H.; Ober, R.; Jensen, K. F.; Bawendi, M. G., (CdSe)ZnS Core-Shell Quantum Dots: Synthesis and Optical and Structural Characterization of a Size Series of Highly Luminescent Materials. *J. Phys. Chem. B* **1997,** *101*, 9463-9475.

3. Milliron, D. J.; Hughes, S. M.; Cui, Y.; Manna, L.; Li, J.; Wang, L.; Alivisatos, A. P., Colloidal Nanocrystal Heterostructures with Linear and Branched Topology. *Nature* **2004,** *430*, 190-195.

4. Boles, M. A.; Ling, D.; Hyeon, T.; Talapin, D. V., The Surface Science of Nanocrystals. *Nat. Mater.* **2016,** *15*, 141-153.

5. Kagan, C. R.; Lifshitz, E.; Sargent, E. H.; Talapin, D. V., Building Devices from Colloidal Quantum Dots. *Science* **2016,** *353*, aa5523-1-aa5523-9.

6. Kagan, C. R.; Murray, C. B., Charge Transport in Strongly Coupled Quantum Dot Solids. *Nat. Nanotechnol.* **2015,** *10*, 1013-1026.

7. Dolzhnikov, D. S.; Zhang, H.; Jang, J.; Son, J. S.; Panthani, M. G.; Chattopadhyay, S.; Shibata, T.; Talapin, D. V., Composition-Matched Molecular "Solders" for Semiconductors. *Science* **2015,** *347*, 425-428.

8. García De Arquer, F. P.; Armin, A.; Meredith, P.; Sargent, E. H., Solution-Processed Semiconductors for Next-Generation Photodetectors. *Nat. Rev. Mater.* **2017,** *2*, 16100.

9. Dai, X.; Zhang, Z.; Jin, Y.; Niu, Y.; Cao, H.; Liang, X.; Chen, L.; Wang, J.; Peng, X., Solution-Processed, High-Performance Light-Emitting Diodes Based on Quantum Dots. *Nature* **2014,** *515*, 96-99.

10. Zhang, H.; Kurley, J. M.; Russell, J. C.; Jang, J.; Talapin, D. V., Solution-Processed, Ultrathin Solar Cells from $CdCl_3^-$-Capped CdTe Nanocrystals: The Multiple Roles of $CdCl_3^-$ Ligands *J. Am. Chem. Soc.* **2016,** *138*, 7464–7467.

11. She, C.; Fedin, I.; Dolzhnikov, D. S.; Dahlberg, P. D.; Engel, G. S.; Schaller, R. D.; Talapin, D. V., Red, Yellow, Green, and Blue Amplified Spontaneous Emission and Lasing Using Colloidal CdSe Nanoplatelets. *ACS Nano* **2015,** *9*, 9475-9485.

12. Braun, E.; Eichen, Y.; Sivan, U.; Ben-Yoseph, G., DNA-Templated Assembly and Electrode Attachment of a Conducting Silver Wire. *Nature* **1998,** *391*, 775-558.

13. Van Gerwen, P.; Laureyn, W.; Laureys, W.; Huyberechts, G.; Op De Beeck, M.; Baert, K.; Suls, J.; Sansen, W.; Jacobs, P.; Hermans, L.; Mertens, R., Nanoscaled Interdigitated Electrode Arrays for Biochemical Sensors. *Sens. Actuators, B* **1998,** *49,* 73-80.

14. Kim, T.; Cho, K.; Lee, E. K.; Lee, S. J.; Chae, J.; Kim, J. W.; Kim, D. H.; Kwon, J.; Amaratunga, G.; Lee, S. Y.; Choi, B. L.; Kuk, Y.; Kim, J. M.; Kim, K., Full-Colour Quantum Dot Displays Fabricated by Transfer Printing. *Nat. Photonics* **2011,** *5*, 176-182.

15. Kurzweil, R., *The Singularity Is Near: When Humans Transcend Biology*. Viking Press: New York, 2005.

16. Choi, J.; Wang, H.; Oh, S. J.; Paik, T.; Sung, P.; Sung, J.; Ye, X.; Zhao, T.; Diroll, B. T.; Murray, C. B.; Kagan, C. R., Exploiting the Colloidal Nanocrystal Library to Construct Electronic Devices. *Science* **2016,** *352*, 205-208.

17. Wood, V.; Panzer, M. J.; Chen, J.; Bradley, M. S.; Halpert, J. E.; Bawendi, M. G.; Bulovic, V., Inkjet-Printed Quantum Dot-Polymer Composites for Full-Color AC-Driven Displays. *Adv. Mater.* **2009,** *21*, 2151-2155.

18. Zhang, H.; Son, J. S.; Dolzhnikov, D. S.; Filatov, A. S.; Hazarika, A.; Wang, Y.; Hudson, M. H.; Sun, C.; Chattopadhyay, S.; Talapin, D. V., Soluble Lead and Bismuth Chalcogenidometallates: Versatile Solders for Thermoelectric Materials. *Chem. Mater.* **2017,** *29*, 6396-6404.

19. Bertino, M. F.; Gadipalli, R. R.; Story, J. G.; Williams, C. G.; Zhang, G.; Sotiriou-Leventis, C.; Tokuhiro, A. T.; Guha, S.; Leventis, N., Laser Writing of Semiconductor Nanoparticles and Quantum Dots. *Appl. Phys. Lett.* **2004,** *85*, 6007-6009.

20. Dogan, S.; Kudera, S.; Dang, Z.; Palazon, F.; Petralanda, U.; Artyukhin, S.; De Trizio, L.; Manna, L.; Krahne, R., Lateral Epitaxial Heterojunctions in Single Nanowires Fabricated by Masked Cation Exchange. *Nat. Commun.* **2018,** *9*, 505.

21. Palazon, F.; Prato, M.; Manna, L., Writing on Nanocrystals: Patterning Colloidal Inorganic Nanocrystal Films through Irradiation-Induced Chemical Transformations of Surface Ligands. *J. Am. Chem. Soc.* **2017,** *139*, 13250-13259.

22. Miszta, K.; Greullet, F.; Marras, S.; Prato, M.; Toma, A.; Arciniegas, M.; Manna, L.; Krahne, R., Nanocrystal Film Patterning by Inhibiting Cation Exchange *via* Electron-Beam or X-Ray Lithography. *Nano Lett.* **2014,** *14*, 2116-2122.

23. Keuleyan, S.; Kohler, J.; Guyot-Sionnest, P., Photoluminescence of Mid-Infrared HgTe Colloidal Quantum Dots. *J. Phys. Chem. C* **2014,** *118*, 2749-2753.

24. Tang, X.; Ackerman, M. M.; Chen, M.; Guyot-Sionnest, P., Dual-Band Infrared Imaging Using Stacked Colloidal Quantum Dot Photodiodes. *Nat. Photonics* **2019,** *13*, 277-282.

25. Chen, Y.; Shih, I., Fabrication of Vertical Channel Top Contact Organic Thin Film Transistors. *Org. Electron.* **2007,** *8*, 655–661.

26. Paskiewicz, D. M.; Sichel-Tissot, R.; Karapetrova, E.; Stan, L.; Fong, D. D., Single-Crystalline $SrRuO_3$ Nanomembranes: A Platform for Flexible Oxide Electronics. *Nano Lett.* **2016**, *16*, 534–542.

27. Khorasaninejad, M.; Chen, W. T.; Devlin, R. C.; Oh, J.; Zhu, A. Y.; Capasso, F., Metalenses at Visible Wavelengths: Diffraction-Limited Focusing and Subwavelength Resolution Imaging. *Science* **2016,** *352*, 1190–1194.

28. Fung, A. O.; Tsiokos, C.; Paydar, O.; Chen, L. H.; Jin, S.; Wang, Y.; Judy, J. W., Electrochemical Properties and Myocyte Interaction of Carbon Nanotube Microelectrodes. *Nano Lett.* **2010,** *10*, 4321–4327.

29. Jiang, L.; Chen, X.; Lu, N.; Chi, L., Spatially Confined Assembly of Nanoparticles. *Acc. Chem. Res.* **2014,** *47*, 3009-3017.

30. Shaw, S.; Yuan, B.; Tian, X.; Miller, K. J.; Cote, B. M.; Colaux, J. L.; Migliori, A.; Panthani, M. G.; Cademartiri, L., Building Materials from Colloidal Nanocrystal Arrays: Preventing Crack Formation During Ligand Removal by Controlling Structure and Solvation. *Adv. Mater.* **2016,** *28*, 8892-8899.

31. Miszta, K.; Greullet, F.; Marras, S.; Prato, M.; Toma, A.; Arciniegas, M.; Manna, L.; Krahne, R., Nanocrystal Film Patterning by Inhibiting Cation Exchange *via* Electron-Beam or X-Ray Lithography. *Nano Lett.* **2014,** *14*, 2116-2122.

32. Palazon, F.; Akkerman, Q. A.; Prato, M.; Manna, L., X-Ray Lithography on Perovskite Nanocrystals Films: From Patterning with Anion-Exchange Reactions to Enhanced Stability in Air and Water. *ACS Nano* **2016,** *10*, 1224-1230.

33. Wang, Y.; Fedin, I.; Zhang, H.; Talapin, D. V., Direct Optical Lithography of Functional Inorganic Nanomaterials. *Science* **2017,** *357*, 385-388.

34. Okamura, H.; Ashida, T.; Kodama, S.; Shirai, M., i-Line Sensitive Pags and Their Application to Photocrosslinking System. *Macromol. Symp.* **2015,** *349*, 29-33.

35. Okamura, H.; Shirai, M., I-Line Sensitive Photoacid Generators. *Trends Photochem. Photobiol.* **2013,** *15*, 51-61.

36. Taylor, J. W.; Bassett, D. R. Dual-Tone Photoresist Utilizing Diazonaphthoquinone Resin and Carbodiimide Stabilizer. U.S. Patent 5087547, 1992.

37. Liaros, N.; Tomova, Z.; Razo, S. a. G.; Cohen, S. R.; Fourkas, J. T.; Wolf, S. M.; Thum, M.; Falvey, D. E.; Ogden, H. M.; Mullin, A. S.; Pranda, A.; Oehrlein, G. S.; Petersen, J. S., The State of the Art in Multicolor Visible Photolithography. *SPIE Proceedings* **2018,** *10584*, 1058407.

38. Jiang, J.; Chakrabarty, S.; Yu, M.; Ober, C. K., Metal Oxide Nanoparticle Photoresists for EUV Patterning. *J. Photopolym. Sci. Tec.* **2014,** *27*, 663-666.

39. Xu, H.; Sakai, K.; Kasahara, K.; Kosma, V.; Yang, K.; Herbol, H. C.; Odent, J.; Clancy, P.; Giannelis, E. P.; Ober, C. K., Metal–Organic Framework-Inspired Metal-Containing Clusters for High-Resolution Patterning. *Chem. Mater.* **2018,** *30*, 4124-4133.

40. Chakrabarty, S.; Ouyang, C.; Krysak, M.; Trikeriotis, M.; Cho, K.; Giannelis, E. P.; Ober, C. K., Oxide Nanoparticle Euv Resists: Toward Understanding the Mechanism of Positive and Negative Tone Patterning. SPIE, **2013**, *8679*, 8.

41. Yu, M.; Giannelis, E. P.; Ober, C. K., Positive Tone Oxide Nanoparticle Euv (One) Photoresists. *Advances in Patterning Materials and Processes XXXIII* **2016,** 977905-1-977905-5.

42. Li, L.; Chakrabarty, S.; Spyrou, K.; Ober, C. K.; Giannelis, E. P., Studying the Mechanism of Hybrid Nanoparticle Photoresists: Effect of Particle Size on Photopatterning. *Chem. Mater.* **2015,** *27*, 5027-5031.

43. Telecky, A.; Xie, P.; Stowers, J.; Grenville, A.; Smith, B.; Keszler, D. A., Photopatternable Inorganic Hardmask. *J. Vac. Sci. Technol.* **2010,** *28*, C6S19-C6S22.

44. Nag, A.; Kovalenko, M. V.; Lee, J.-S.; Liu, W.; Spokoyny, B.; Talapin, D. V., Metal-Free Inorganic Ligands for Colloidal Nanocrystals: S^{2-}, HS^{-}, Se^{2-}, HSe^{-}, Te^{2-}, HTe^{-}, TeS_3^{2-}, OH^{-}, and NH_2^{-} as Surface Ligands. *J. Am. Chem. Soc.* **2011,** *133*, 10612-10620.

45. Huang, J.; Liu, W.; Dolzhnikov, D. S.; Protesescu, L.; Kovalenko, M. V.; Koo, B.; Chattopadhyay, S.; Shenchenko, E. V.; Talapin, D. V., Surface Functionalization of Semiconductor and Oxide Nanocrystals with Small Inorganic Oxoanions (PO_4^{3-}, MoO_4^{2-}) and Polyoxometalate Ligands. *ACS Nano* **2014,** *8*, 9388-9402.

46. Debnath, R.; Tang, J.; Barkhouse, D. A.; Wang, X.; Pattantyus-Abraham, A. G.; Brzozowski, L.; Levina, L.; Sargent, E. H., Ambient-Processed Colloidal Quantum Dot Solar

Cells *via* Individual Pre-Encapsulation of Nanoparticles. *J. Am. Chem. Soc.* **2010,** *132*, 5952-5953.

47. Dubois, F.; Mahler, B.; Dubertret, B.; Doris, E.; Mioskowski, C., A Versatile Strategy for Quantum Dot Ligand Exchange. *J. Am. Chem. Soc.* **2007,** *129*, 482-283.

48. Frederick, M. T.; Amin, V. A.; Cass, L. C.; Weiss, E. A., A Molecule to Detect and Perturb the Confinement of Charge Carriers in Quantum Dots. *Nano Lett.* **2011,** *11*, 5455-5460.

49. Leonov, A. P.; Wei, A., Photolithography of Dithocarbamate-Anchored Monolayers and Polymers on Gold. *J. Mater. Chem.* **2011,** *21*, 4371-4376.

50. Kovalenko, M. V.; Bodnarchuk, M. I.; Zaumseil, J.; Lee, J.; Talapin, D. V., Expanding the Chemical Versatility of Colloidal Nanocrystals Capped with Molecular Metal Chalcogenide Ligands. *J. Am. Chem. Soc.* **2010,** *132*, 10085-10092.

51. Kovalenko, M. V.; Scheele, M.; Talapin, D. V., Colloidal Nanocrystals with Molecular Metal Chalcogenide Surface Ligands. *Science* **2009,** *324*, 1417-1420.

52. Nag, A.; Chung, D. S.; Dolzhnikov, D. S.; Dimitrijevic, N. M.; Chattopadhyay, S.; Shibata, T.; Talapin, D. V., Effect of Metal Ions on Photoluminescence, Charge Transport, Magnetic and Catalytic Properties of All-Inorganic Colloidal Nanocrystals and Nanocrystal Solids. *J. Am. Chem. Soc.* **2012,** *134*, 13604-13615.

53. Bellerby, J. M., The Chemical Effects of Storing Hydrazine Containing Carbon Dioxide Impurity in Stainless Steel Systems. *J. Hazard. Mater.* **1983,** *7*, 187-197.

54. Hahnkamm, V.; Kiel, G.; Gattow, G., Chalcogen Carbonates. Xxxi. Polymorphism of Ammonium Dithiocarbamate. *Naturwissenschaften* **1968,** *55*, 80-81.

55. Joris, S. J.; Aspila, K. I.; Chakrabarti, C. L., On the Mechanism of Decomposition of Dithiocarbamates. *J. Phys. Chem.* **1970,** *74*, 860-865.

56. Losanitch, S. M., Ccciii.—Decomposition of Dithiocarbazinates. *J. Chem. Soc., Trans.* **1922,** *121*, 2542-2545.

57. Nesmerak, K.; Pospisek, M.; Nemec, I.; Waisser, K.; Gabriel, J., Antifungal Properties of Substituted 1-Phenyl-5-Mercaptotetrazoles and Their Oxidation Product, 5-Bis-(1-Phenyltetrazolyl)Disulfide. *Folia Microbiologica* **2000,** *45*, 138-142.

58. Foldenyi, R., New 1h-Tetrazole-5-Thiol Derivatives as Pesticides. II. Cyanodithioimidocarbonic Acid Esters. *Monatshefte fuer Chemie* **1995,** *126*, 1035-1043.

59. Dunkin, I. R.; Shields, C. J.; Quast, H., The Photochemistry of 1,4-Dihtdro-5h-Tetrazole Derivatives Isolated in Low-Temperature Matrices. *Tetrahedron* **1989,** *45*, 259-268.

60. Voitekhovich, S. V.; Talapin, D. V.; Klinke, C.; Kornowski, A.; Weller, H., Cds Nanoparticles Capped with 1-Substituted 5-Thiotetrazoles: Synthesis, Characterization, and Thermolysis of the Surfactant. *Chem. Mater.* **2008,** *20*, 4545-4547.

61. Voitekhovich, S. V.; Lesnyak, V.; Gaponik, N.; Eychmuller, A., Tetrazoles: Unique Capping Ligands and Precursors for Nanostructured Materials. *Small* **2015,** *11*, 5728-5739.

62. Maier, G.; Eckwert, J.; Bothur, A.; Reisenauer, H. P.; Schmidt, C., Photochemical Fragmentation of Unsubstituted Tetrazole 1,2,3-Triazole, and 1,2,4-Triazole. First Matrix-Spectroscopic Identification of Nitrilimine HCNNH. *Liebigs Ann* **1996**, 1041-1053.

63. Pagacz-Kostrzewa, M.; Krupa, J.; Wierzejewska, M., Photochemical Transformations of 5-Methyltetrazole. Matrix Isolation FTIR and DFT Studies. *J. Photochem. Photobiol. A* **2014,** *277*, 37-44.

64. Alawode, O. E.; Robinson, C.; Rayat, S., Clean Photodecomposition of 1-Methyl-4-Phenyl-1h-Tetrozole-5(4h)-Thiones to Carbodiimides Proceeds *via* a Biradical. *J, Org. Chem.* **2011,** *76*, 216-222.

65. Al-Shakban, M.; Matthews, P. D.; Deogratias, G.; Mcnaughter, P. D.; Raftery, J.; Vitorica-Yrezabal, I.; Mubofu, E. B.; O'brien, P., Novel Xanthate Complexes for the Size-Controlled Synthesis of Copper Sulfide Nanorods. *Inorg. Chem.* **2017,** *56*, 9247-9254.

66. Lewis, E. A.; Mcnaughter, P. D.; Yin, Z.; Chen, Y.; Brent, J. R.; Saah, S. A.; Raftery, J.; Awudza, J. a. M.; Malik, M. A.; O'brien, P.; Haigh, S. J., *In Situ* Synthesis of Pbs Nanocrystals in Polymer Thin Films from Lead(II) Xanthate and Dithiocarbamate Complexes: Evidence for Size and Morphology Control. *Chem. Mater.* **2015,** *27*, 2127-2136.

67. Nair, P. S.; Scholes, G. D., Thermal Decomposition of Single Source Precursors and the Shape Evolution of CdS and CdSe Nanocrystals. *J. Mater.Chem.* **2006,** *16*, 467-473.

68. Dietzsch, W.; Strauch, P.; Hoyer, E., Thio-Oxalates: Their Ligand Properties and Coordination Chemistry *Coord. Chem. Rev.* **1992,** *121*, 43-130.

69. Bernt, C. M.; Burks, P. T.; Demartino, A. W.; Pierri, A. E.; Levy, E. S.; Zigler, D. F.; Ford, P. C., Photocatalytic Carbon Disulfide Production *via* Charge Transfer Quenching of Quantum Dots. *J. Am. Chem. Soc.* **2014,** *136*, 2192-2195.

70. Tipman, R. N.; Leja, J., Reactivity of Xanthate and Dixanthogen in Aqueous Solutions of Different pH. *Colloid Polym. Sci* **1975,** *253*, 4-10.

71. Dong, A.; Ye, X.; Chen, J.; Kang, Y.; Gordon, T.; Kikkawa, J. M.; Murray, C. B., A Generalized Ligand-Exchange Strategy Enabling Sequential Surface Functionalization of Colloidal Nanocrystals. *J. Am. Chem. Soc.* **2011,** *133*, 998-1006.

72. Doris, S. E.; Lynch, J. J.; Li, C.; Wills, A. W.; Urban, J. J.; Helms, B. A., Mechanistic Insight into the Formation of Cationic Naked Nanocrystals Generated under Equilibrium Control. *J. Am. Chem. Soc.* **2014,** *136*, 15702–15710.

73. Rosen, E. L.; Buonsanti, R.; Llordes, A.; Sawvel, A. M.; Milliron, D. J.; Helms, B. A., Exceptionally Mild Reactive Stripping of Native Ligands Fromnanocrystal Surfaces by Using Meerwein's Salt. *Angew. Chem. Int. Ed.* **2012,** *51*, 684-689.

74. Shirai, M.; Tsunooka, M., Photoacid and Photobase Generators: Chemistry and Applications to Polymeric Materials. *Prog. Polym. Sci.* **1996,** *21*, 1-45.

75. Crivello, J. V., The Discovery and Development of Onium Salt Cationic Photoinitiators. *J. Polym. Sci. A* **1999,** *37*, 4241-4254.

76. Watt, W. R.; Hoffman Jr, H. T.; Pobiner, H.; Schkolnick, L. J.; Yang, L. S., A Novel Photoinitiator of Cationic Polymerization: Preparation and Characterization of Bis [4-(Diphenylsulfonio)Phenyl]Sulfide–Bis-Hexafluorophosphate. *J. Polym. Sci. A* **1984,** *22*, 1789-1796.

77. Bratton, D.; Ayothi, R.; Deng, H.; Cao, H. B.; Ober, C. K., Diazonaphthoquinone Molecular Glass Photoresists: Patterning without Chemical Amplification. *Chem. Mater.* **2007,** *19*, 3780-3786.

78. Dammel, R. R., *Diazonaphthoquinone-Based Resists*. SPIE: San Francisco, 1993.

79. Drano, Y.; Miyazaki, M.; Katsuya, K.; Kikugh, H., DNQ-Pac Structure: 4-, 5- and 6-Sulfonyl DNQ Ester. *J. Photopolym. Sci. Tec.* **1993,** *6*, 53-56.

80. Zhang, J.; Xiao, P.; Morlet-Savary, F.; Graff, B.; Fouassiera, J. P.; Lalevée, J., A Known Photoinitiator for a Novel Technology: 2-(4-Methoxystyryl)-4, 6-Bis (Trichloromethyl)-1, 3, 5-Triazine for Near UV or Visible LED. *Polym. Chem.* **2014,** *5*, 6019-6026.

81. Li, L.; Chakrabarty, S.; Spyrou, K.; Ober, C. K.; Giannelis, E. P., Studying the Mechanism of Hybrid Nanoparticle Photoresists: Effect of Particle Size on Photopatterning. *Chem. Mater.* **2015,** *27*, 5027-5031.

82. Capello, C.; Fischer, U.; Hungerbuhler, K., What Is a Green Solvent? A Comprehensive Framework for the Environmental Assessment of Solvents. *Green Chem.* **2007,** *9*, 927-934.

83. Liu, W.; Howarth, M.; Greytak, A. B.; Zheng, Y.; Nocera, D. G.; Ting, A. Y.; Bawendi, M. G., Compact Biocompatible Quantum Dots Functionalized for Cellular Imaging. *J. Am. Chem. Soc.* **2008,** *130* , 1274-1284.

84. Kim, W. J.; Kim, S. J.; Lee, K.; Samoc, M.; Cartwright, A. N.; Prasad, P. N., Robust Microstructures Using UV Photopatternable Semiconductor Nanocrystals. *Nano Lett.* **2008,** *8*, 3262-3265.

85. Buchwald, K., Fused Silica Transmission Gratings *Ibsen Photonics,* https://ibsen.com/wp-content/uploads/White-paper-Fused-Silica-Transmission-Gratings-v1.0.pdf, (accessed October **2019**).

86. Alqattan, B.; Yetisen, A. K.; Butt, H., Direct Laser Writing of Nanophotonic Structures on Contact Lenses. *ACS Nano* **2018,** *12*, 5130-5140.

87. Jiang, H.; Kaminska, B., Scalable Inkjet-Based Structural Color Printing by Molding Transparent Gratings on Multilayer Nanostructured Surfaces. *ACS Nano* **2018,** *12*, 3112-3125.

88. Enomoto, K.; Moon, S.; Maekawa, Y.; Shimoyama, J.; Goto, K.; Narita, T.; Yoshida, M., Novel Electron-Beam-Induced Reaction of a Sulfonium Salt in the Solid State. *J. Vac. Sci. Technol. B* **2006,** *24*, 2337-2349.

89. Gangnaik, A. S.; Georgiev, Y. M.; Holmes, J. D., New Generation Electron Beam Resists: A Review. *Chem. Mater.* **2017,** *29*, 1898-1917.

90. Yang, W. C.; Huang, Y. S.; Shew, B. Y.; Fu, C. C., Study on Diffraction Effect and Microstructure Profile Fabricated by One-Step Backside Lithography. *J. Micromech. Microeng.* **2013,** *23*, 035004.

91. Maekawa, Y.; Yuasa, K.; Enomoto, K.; Matsushita, H.; Kato, J.; Yamashita, T.; Itoh, K.; Yoshida, M., Electron-Beam-Induced Color Imaging of Acid-Chromic Polymer Films. *Chem. Mater.* **2008,** *20*, 5320-5324.

92. Shimoni, O.; Cervenka, J.; Karle, T. J.; Fox, K.; Gibson, B. C.; Tomljenovic-Hanic, S.; Greentree, A. D.; S., P., Development of a Templated Approach to Fabricate Diamond Patterns on Various Substrates. *ACS Appl. Mater. Interfaces* **2014,** *6*, 8894-8902.

93. Nandwana, V.; Subramani, C.; Yeh, Y.-C.; Yang, B.; Dickert, S.; Barnes, M. D.; Tuominen, M. T.; Rotello, V. M., Direct Patterning of Quantum Dot Nanostructures *via* electron Beam Lithography. *J. Mater. Chem.* **2011,** *21*, 16859-16862.

94. Ayothi, R.; Yi, Y.; Cao, H. B.; Wang, Y.; Putna, S.; Ober, C. K., Arylonium Photoacid Generators Containing Environmentally Compatible Aryloxyperfluoroalkanesulfonate Groups. *Chem. Mater.* **2007,** *19*, 1434-1444.

95. Tobing, L. Y. M.; Tjahjana, L.; Zhang, D. H., Direct Patterning of High Density Sub-15 nm Gold Dot Arrays Using Ultrahigh Contrast Electron Beam Lithography Process on Positive Tone Resist. *Nanotechnology* **2013,** *24*, 075303.

96. Gangnaik, A. S.; Georgiev, Y. M.; Holmes, J. D., New Generation Electron Beam Resists: A Review. *Chem. Mater.* **2017,** *29*, 1898-1917.

Table of Contents Graphic